Optimization of the Scan Protocol for the Reduction of Diaphragmatic Motion Artifacts Depicted on CT Angiography: a Phantom Study Simulating Pediatric Patients with Free Breathing

Jee Hyun Baek, MD
Whal Lee, MD
Kee-Hyun Chang, MD
Jin Wook Chung, MD
Jae Hyung Park, MD

All authors: Department of Radiology,
Seoul National University College of
Medicine, Institute of Radiation Medicine,
Seoul National University Medical
Research Center, and Clinical Research
Institute, Seoul National University
Hospital, Seoul 110-744, Korea

Address reprint requests to:
Whal Lee, MD, Department of Radiology,
Seoul National University Hospital, 101
Daehang-ro, Jongno-gu, Seoul 110-744,
Korea.
Tel. (822) 2072-2584
Fax. (822) 743-6385
e-mail: leew@radiol.snu.ac.kr

Objective: This study was designed to optimize the scan protocol of CT angiography to reduce diaphragmatic motion artifacts in pediatric patients with free-breathing.

Materials and Methods: A phantom with twelve tubes with different diameters was constructed. To simulate free-breathing, the phantom was connected to a motor, and the phantom moved along the axis of scan. Scans were performed under several conditions: different pitch (1, 1.5) and gantry rotation time (0.37 and 0.75 sec), and different movement range (1 cm, 3 cm) and rates (20/min, 40/min). For CT scanning, a 16-channel CT scanner was used and fixed factors of the CT protocol were as follows: 100 effective mAs, 80 kVp, reconstruction with a soft-algorithm, beam collimation 16×75 mm, reconstruction thickness of 1 mm, and an interval of 0.5 mm. CT scans were repeated five times. Each tube was evaluated with the use of a grading system (0 for images where tubes were not discriminable and 2 for images where tubes were clearly discriminable).

Results: A higher pitch and shorter gantry rotation time produced images with a higher grade. Average grades for the higher pitch (1.5) and faster gantry rotation time (0.37 sec) for each combination of movement were as follows: 1.94 (range 1 cm and rate 20/min), 1.42 (range 1 cm and rate 40/min), 0.86 (range 3 cm and rate 20/min) and 0.52 (range 3 cm and rate 40/min). Average grades for the lower pitch (1) and slower gantry rotation time (0.75 sec) for each combination of movement were 1.08, 0.56, 0.32 and 0.08, respectively.

Conclusion: The scanning speed and especially the pitch are important parameters for CT scans to overcome a respiratory motion artifact.

Computed tomography (CT) angiography is able to produce high quality images for the noninvasive assessment of vascular anatomy for patients with complex congenital heart disease (1, 2). The feasibility of CT angiography (CTA) has made the modality an important imaging tool for the diagnosis and follow-up of both young and old patients with vascular disease. There has been substantial information reported about the imaging techniques and scan protocols for CTA in adults, but little information is available for CTA in children. Children are different from adults for such features as body size, circulation time, respiratory cycle and breath-holding ability. To the best of our knowledge, there has been no study that has described a proper scan protocol in combination with the various factors related to scanning speed.

The purpose of this study was to reveal the relationship between factors for CT

scanning and artifacts from periodic movement and to help determine appropriate scan protocols of CTA for children who cannot hold their breath.

MATERIALS AND METHODS

The present study was performed only with a phantom and no Institutional Review Board approval was required.

The Phantom

We constructed a phantom model that mimicked normal vessels and vessels with stenosis in this study. We intended to simulate the condition of a CT scan of the pulmonary arteries and partly aortic arch as these two components are connected to the heart and are influenced by cardiac and diaphragmatic motion. The outer cage was an open-top box made of acryl plates, inside of which 12 polyethylene tubes with variable diameters were placed; the largest tube for flow supply lay along the long axis of the cage and 11 smaller tubes branched out. Ten tubes for the main experimental study were connected at right angles with the

Fig. 1. Image of phantom tube obtained with use of Faxitron X-ray system. For accurate measurement of diameter of tubes, we used four types of round 'reference metal bearings (*)' of variable size that were already measured. In descending order of size, diameters of bearings are 1/4 inch, 3/16 inch, 1/8 inch and 5/32 inch (1 inch = 25.4 mm).
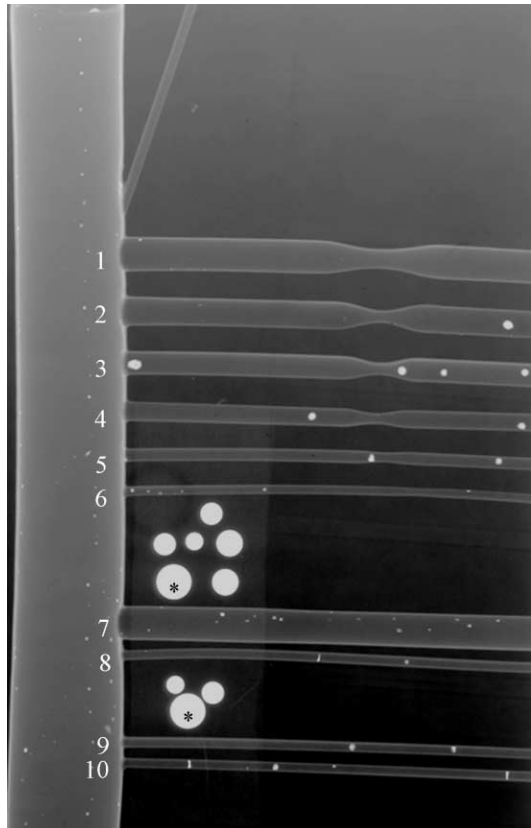
largest tube and ran parallel to each other; six of the tubes had stenotic segments that were not analyzed in the present study. The last tube branched obliquely from the largest tube and landed at the wall of the cage.

To measure precisely the inner diameters of the tubes, radiographs of the vascular phantom were obtained with a Hewlett Packard Faxitron X-ray system (model 43805N; Hewlett Packard, Palo Alto, CA) with a tube potential of 70 kVp for 90 seconds using Kodak X-OMAT scientific imaging film (Eastman Kodak, Rochester, NY) (Fig. 1). The Faxitron X-ray system was used in place of computed radiography or digital radiography equipment currently available in our hospital. The values of the inner diameters of the tubes were measured and results are listed in Table 1.

The phantom vessels were filled with a mixture of contrast media (Ultravist 370; Schering, Berlin, Germany) and normal saline in the ratio of 1.7:100. The targeted CT number in the largest tube was about 300 (3, 4). The residual space of the cage was filled with distilled water to decrease beam-hardening artifacts and to obtain images with good contrast. The phantom was placed on the moving table of the CT unit with the long axis parallel to the axis of scanning (Fig. 2A, B).

Simulation of Respiratory Movement with the Phantom

To simulate the breathing movement of children, the phantom was connected to a small ventilator (DJ-4025, Daejong Instrument Industry, Seoul, Korea) with a plastic arm. The phantom was moved parallel to the axis of scanning to mimic the diaphragmatic movements of children during a CT scan.

Table 1. Inner Diameters of Tubes Measured from Radiographs of Vascular Phantom

No	Diameter (mm) Patent Segment	Stenotic Segment*
1	5.7	3.1
2	4.6	1.8
3	3.9	1.6
4	3.2	1.5
5	1.9	1.8
6	1.3	1.0
Diameter (mm) of Tubes without Stenosis		
7		5.8
8		1.5
9		1.5
10		1.4

Note.— Tube numbers are identical as described in Figure 1. First to sixth tubes have stenotic portions in mid segments. Seventh to tenth tubes have no stenoses. Stenotic segments (*) were not analyzed in this study.

Five conditions were applied to simulate breathing movement of children of various ages and body sizes. Images with no movement were acquired first, and then the phantom was moved back and forth in four combinations: a combination of 1 cm and 3 cm for amplitude, and 20 revolutions per minute (RPM) and 40 RPM for the rotating arm of the small ventilator to simulate respiration with a different rate (Table 2). In a pilot study, CT scanning of the phantom with a higher RPM such as 60 RPM did not provide images with sufficient quality for analysis.

The actual velocity of the phantom movement was calculated by adding the scan speed and phantom velocity. The velocity of phantom movement could be obtained from the angular velocity of the rotating arm of the small ventilator.

Imaging Protocol
A CT instrument with 16 channel detectors (SOMATOM Sensation16; Siemens Medical Solutions, Enlangen, Germany) was used for scanning. The fixed factors of the CT protocol were as follows: 100 effective mAs, 80 kVp, B30 kernel for a soft tissue algorithm, beam collimation of 16×0.75 mm, reconstruction thickness of 1 mm and reconstruction interval of 0.5 mm. The effective milliampere second, as defined by Mahesh et al. (5), corresponded to milliampere second divided by the pitch, where pitch is defined by Silverman et al. (6) as the ratio between the table feed per rotation and the X-ray beam width. The resultant radiation dose for each session of a CT scan with an effective 100 mAs and 80 kVp was 2.60 or 2.61 mGy.

The variable parameters of the CT scan were as follows: a pitch of 1 and 1.5; gantry rotation time of 0.37 and 0.75 seconds. Four conditions were applied to each of the movement conditions (Table 3). Based on parameters including the table feed and gantry rotation time, the scanning speed (7) or table speed were calculated using the

Table 2. Five Conditions of Phantom Movement for Simulation of Respiration

Amplitude	Rate
0 cm	0 RPM* (no movement)
1 cm	20 RPM
1 cm	40 RPM
3 cm	20 RPM
3 cm	40 RPM

Note.— When phantom did not move, images were of sufficient quality to differentiate all tubes regardless of pitch and gantry rotation time.
*RPM = revolutions per minute

Table 3. Four Conditions of Scanning Speed with Varying Pitch and Gantry Rotation Time

Pitch	Gantry Rotation Time	Scanning Speed (cm/sec)
1	0.75 sec	1.6
1.5	0.75 sec	2.4
1	0.37 sec	3.2
1.5	0.37 sec	4.8

Note.— For 16 channel multidetector CT scanner with 0.75 mm detector width used in this study, beam collimation width was 12 mm. Scanning speed could be calculated by multiplying beam collimation width by pitch and dividing total by gantry rotation time.


A

Fig. 2. Phantom model placed on CT and corresponding maximum intensity projection image.
A. Phantom is connected to small ventilator and placed on CT table.
B. Example of maximum intensity projection image. Maximum intensity projection image was reconstructed using commercially available software from 1 mm-thickness axial images with scan condition of pitch 1.5-gantry rotation 0.37 sec and no movement of phantom.
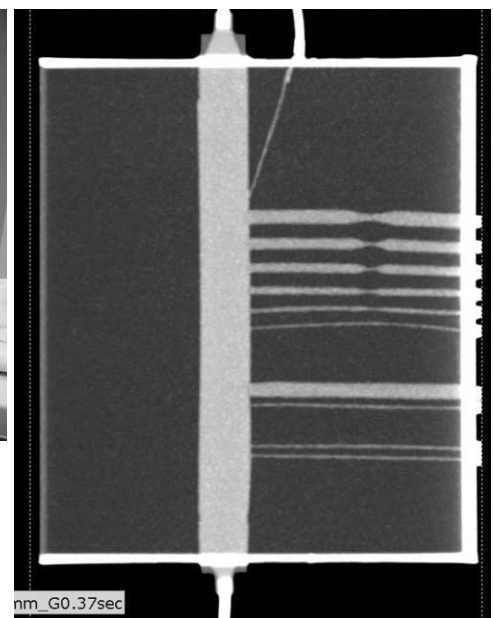
B

following equation:

$$\text{Table speed (mm/sec or cm/sec)} = \frac{\text{Table feed}}{\text{Gantry rotation time}}$$

The values of scanning speed for each condition of pitch and gantry rotation are shown in Table 3.

Scanning of the Phantom and Maximum Intensity Projection Images Reconstruction

In one session of CT scanning, 17 datasets were acquired; one dataset with no movement of the phantom and an additional 16 datasets, including four sets of CT scanning conditions times four sets of phantom movement conditions. To avoid erroneous factors of the CT instrument, five sessions of CT scanning were performed on five different days.

For each scan condition, one coronal plane maximum intensity projection (MIP) image with a 10 mm thickness was created from the axial source images using a stand-alone three-dimensional reconstruction program (Rapidia,

INFINITT Technology, Seoul, Korea). These coronal plane MIP images displayed all of the tubes in the phantom and the effect of motion was analyzed with the use of these images.

Image Analysis

As a result of the five sessions of CT scanning, we obtained five sets of MIP images for each of the 17 scan conditions. Twenty images under conditions of no movement of the phantom were excluded as they all displayed images with good quality. Eventually, eighty images were included in the analysis.

The image quality of the tubes, especially the sharpness of the tubes on each MIP image, was evaluated with the use of a scoring system. Score 2 was designated when the outer margin was clear and each tube was discernable; score 1 was designated when each tube could be separated from the adjacent tubes but the outer margin was blurred; score 0 was designated when a motion artifact was so severe as not to permit the discrimination of one tube from the next tube (Fig. 3). The image analysis was performed

A   **B**

C   **D**
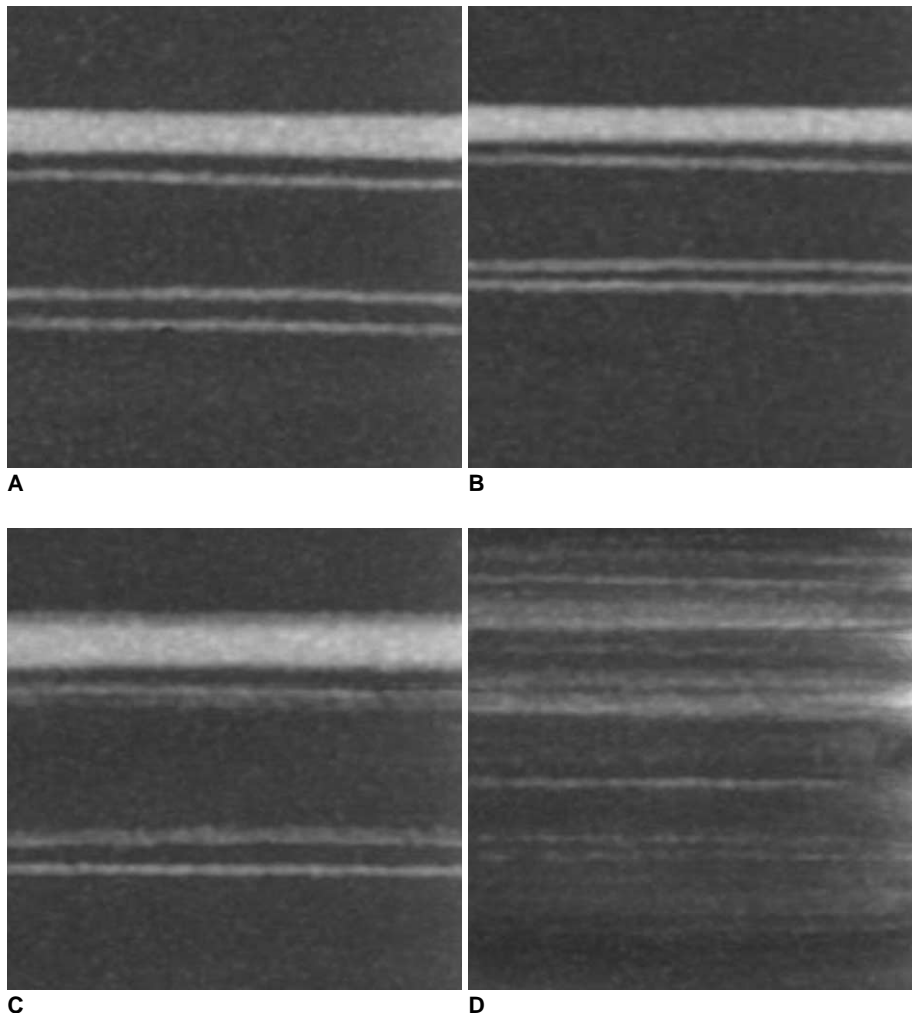
Fig. 3. Representative phantom tubes for each score of non-stenotic tubes (#7−10 in Fig. 1) under different scan conditions and phantom movement conditions.
A. Maximum intensity projection image of tubes with no movement of phantom shows clear margins of all tubes.
B. Maximum intensity projection image of tubes for condition of pitch 1.5-gantry rotation 0.37 sec and amplitude 1 cm-20 RPM. All of tubes show clear margins, with score of 2.
C. Maximum intensity projection image of tubes for condition of pitch 1-gantry rotation 0.37 sec and amplitude 1 cm-20 RPM. All of tubes are discernable, but margins of upper three tubes are not as clear as described in (**B**) and are scored 1.
D. Maximum intensity projection image of tubes for condition of pitch 1-gantry rotation 0.75 sec and amplitude 3 cm-40 RPM. Margins of tubes are not clear and tubes cannot be separated from each other, and are scored 0.

by two cardiovascular radiologists blinded to information about the scan conditions. For each of the 16 scan conditions, scores for the tubes at the same location in five images were processed to obtain average values.

RESULTS

To evaluate imaging quality, we selected the largest tube without stenosis (the #7 tube), measured the apparent diameter, calculated the average and standard deviation. The mean CT number of the central tube was 290.4 with one standard deviation of 16.0 (CT number range: 252–323). For all scan conditions, the central tube was clearly discerned from the surrounding water. Six tubes with stenoses were laid so close to one another that the outer margins overlapped, and three tubes without stenoses

were too small to measure the diameter in every scan condition without creating a significant error.

For each scan condition, the velocity as a sum of the scanning speed or table speed (which always had a positive value, as the table moves away from the detector during the scan) and the velocity of phantom movement (which can have a negative value as for some part of the movement, the phantom moves closer to the detector during the scan) were calculated and are graphed as shown in Figures 4 and 5. In Figure 4, four curves with the same velocity of the phantom and different scanning speeds are shown. The shape of the curve reflects the velocity of the phantom and the beginning point of each of the four graphs represents the scanning speed for each scan condition; curves with a higher pitch and shorter time of gantry rotation (i.e. a higher scanning speed) are located at
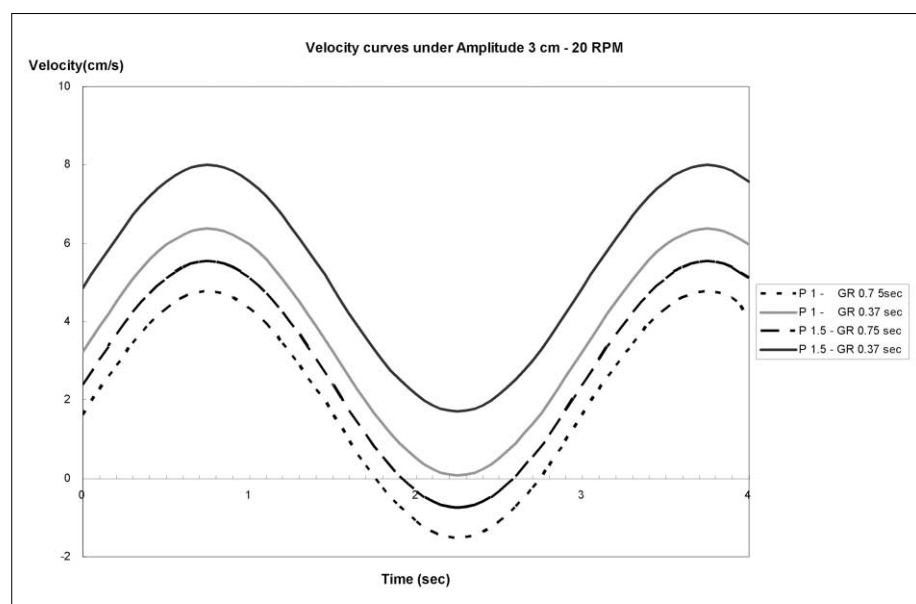
Fig. 4. Velocity curves for phantom movement with different scanning speeds (different pitches and gantry rotation times) for condition amplitude 3 cm-20 RPM, with ground as a reference point. P = Pitch, GR = gantry rotation time
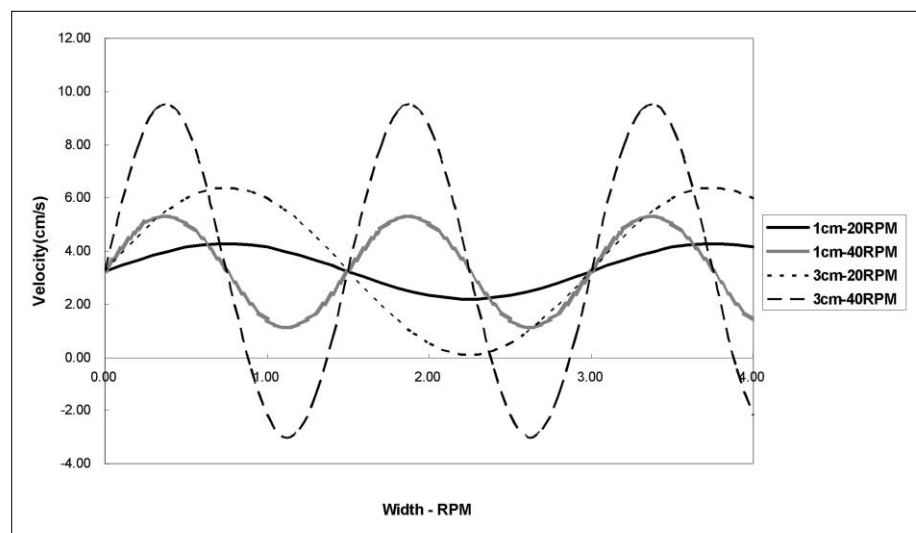
Fig. 5. Velocity curves for phantom movement with pitch 1 and gantry rotation time 0.37 sec. With increase of amplitude and rate of phantom movement, velocity curves show higher amplitude and frequency.

a higher level. All four graphs show the same shape as the amplitude and rate of the movement of the phantom does not change, but the scanning speed does change. As the scanning speed increases, segments with negative velocity of the phantom decrease or disappear. Thus, the phantom does not move close to the detector.

In Figure 5, four curves with different phantom speeds and same scanning speed are presented. A wider range of motion and faster movement rate are reflected as a higher amplitude and frequency of the curve. Each curve represents each condition of phantom movement with same scanning speed of 3.2 cm/sec (pitch 1 and gantry rotation time, 0.37 sec). The curve for the fastest movement of the phantom (amplitude 3 cm and 40 RPM) has segments with a negative value, which indicates that the phantom actually moves towards the detector in the opposite direction of the table movement.

After scanning, image data were acquired and processed

to produce MIP images. As the speed of the phantom movement increased, the motion artifact became more remarkable. The averaged scores of sharpness of the tubes for each scan condition are tabulated in Table 4.

With a relatively slow movement of phantom, in cases of amplitude 1 cm-rate 20 RPM and amplitude 1 cm-rate 40 RPM, as the speed of CT scanning increased, the overall scores increased, indicating that the quality of images (sharpness of the tubes) improved as the scan speed increased (Fig. 6). As the phantom moved faster, as with the case of amplitude 3 cm-rate 20 RPM and amplitude 3 cm-rate 40 RPM, even though the scan speed increased, there was a decrease of scores from 0.9 (3 cm and 20 RPM) and 0.43 (3 cm and 40 RPM) with the scan condition of 1.5 pitch-0.75 sec to 0.43 (3 cm and 20 RPM) and 0.27 (3 cm and 40 RPM) with the condition of 1 pitch-0.37 sec.
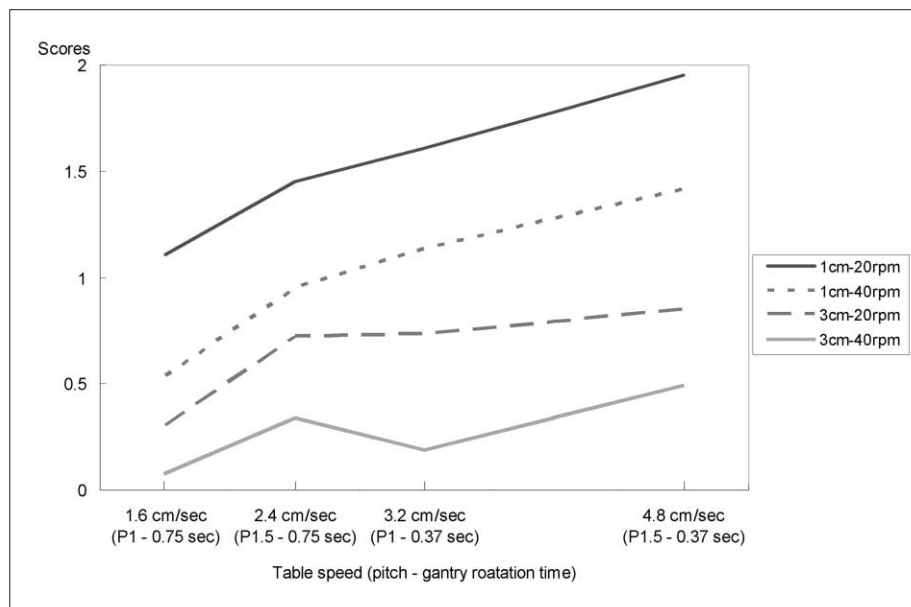
For phantom movement with the condition of amplitude 1 cm-rate 20 RPM and various CT scan conditions,

Table 4. Average Scores of Image Quality of the Phantom Tubes

Five Conditions of Phantom Movement	CT Scan Condition: Scan Speed (pitch-gantry rotation time)			
	1.6 cm/sec (1−0.75 sec)	2.4 cm/sec (1.5−0.75 sec)	3.2 cm/sec (1−0.37 sec)	4.8 cm/sec (1.5−0.37 sec)
No movement	2	2	2	2
1 cm−20 RPM[†]	1.08	1.46	1.64	1.94
1 cm−40 RPM	0.56	0.96	1.12	1.42
3 cm−20 RPM	0.32	0.76	0.68*	0.86
3 cm−40 RPM	0.08	0.36	0.20*	0.52

Note.— Results are averaged values of scores obtained from five times of phantom scanning for each condition of phantom movement and pitch-gantry rotation. For condition of amplitude 3 cm-20 RPM and amplitude 3 cm-40 RPM, scores (*) for condition of 3.2 cm/sec scan speed (pitch 1 and gantry rotation 0.37 sec) are lower than for condition of 2.4 cm/sec scan speed (pitch 1.5 and gantry rotation 0.75 sec).

[†]RPM = revolutions per minute

Fig. 6. Graphs of average scores of image quality of tubes for each scan condition are shown. In general, average score increases as scanning speed increases. For phantom movement of amplitude 3 cm-20 RPM and 40 RPM, scores with scanning speed of 3.2 cm/sec (pitch 1-gantry rotation 0.37 sec) are lower than scores for scanning speed of 2.4 cm/sec (pitch 1.5-gantry rotation 0.75 sec).

measured diameters (averages and standard deviations) of the largest tube without stenosis are shown in Figure 7. As the scan speed increased, the average values approached the true value of 5.87 mm and the standard deviation showed a minimum value at a table speed of 4.8 cm/sec.

DISCUSSION

For CT scanning, one of the main differences between adults and children is breath-holding ability. Breath holding is a great advantage and misregistration caused by respiration seriously degrades the image quality of CTA (8). For heart rate, a study by Ko et al. (9) did not show a linear relationship for heart rate and motion artifacts of great vessels.

We assumed that two components-direction and speed-of object movement contribute to the generation of artifacts along the axis of scanning. In this study, the axis of phantom movement was aligned to the direction of CT scanning and thus we analyzed only longitudinal movement.

The speed of the object-in our study, the phantom-is made up of two components. One component is the speed or velocity of the CT table, or scanning speed, and the other component is the velocity of the phantom movement itself.

The speed of the CT table is constant for each condition of table pitch and gantry rotation time. On the contrary, the velocity of phantom movement follows some rules and is not constant as the arms of the ventilator make a circular movement that is converted to the linear movement of the phantom. Therefore the phantom moves with varying velocity and this movement causes various kinds of misregistration artifacts.

Examples of misregistration due to a motion artifact seen in images from this study are shown in Figure 8. As seen in Figure 8A, when the phantom lay on the CT table and did not move, the image with even the fastest scanning speed did not show noticeable blurring of the tubes. This was an ideal situation for CT scanning.

When the phantom moved in the same direction as that of the CT table, the time for the detector of CT machine to scan the object from the beginning to the end was shorter than for without phantom movement, and the length of the object was considered to be shorter than the actual length (Fig. 8B). When the phantom moved to the opposite direction to that of the CT table and the absolute value of the velocity of the phantom movement was smaller than that of CT table, the time for the detector of the CT machine to scan the object was longer than necessary as the object remained in the scan range for a longer time than required (Fig. 8C). In an extreme case where the velocity of the phantom movement in the opposite direction was faster than the scanning speed, part of the object was actually scanned more than once and part of the object was seen two times or more frequently on the image (Fig. 8D).

In this study, when the phantom moved slowly for the
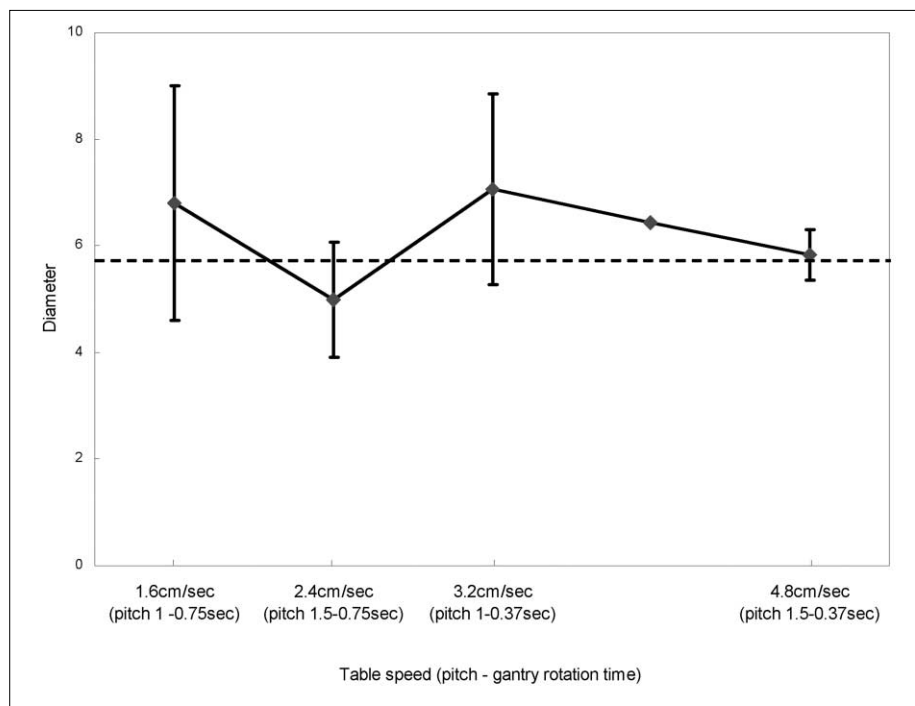
Fig. 7. Averages and standard deviations of measured diameter of #7 tube without stenosis for condition of 1 cm−20 RPM are presented. Dotted line marks true value of tube diameter, 5.82 mm, measured from high resolution plain radiograph of phantom. As scanning speed increases, average values of measured diameter approach true value. Standard deviation shows minimum value at scanning speed of 4.8 cm/sec.
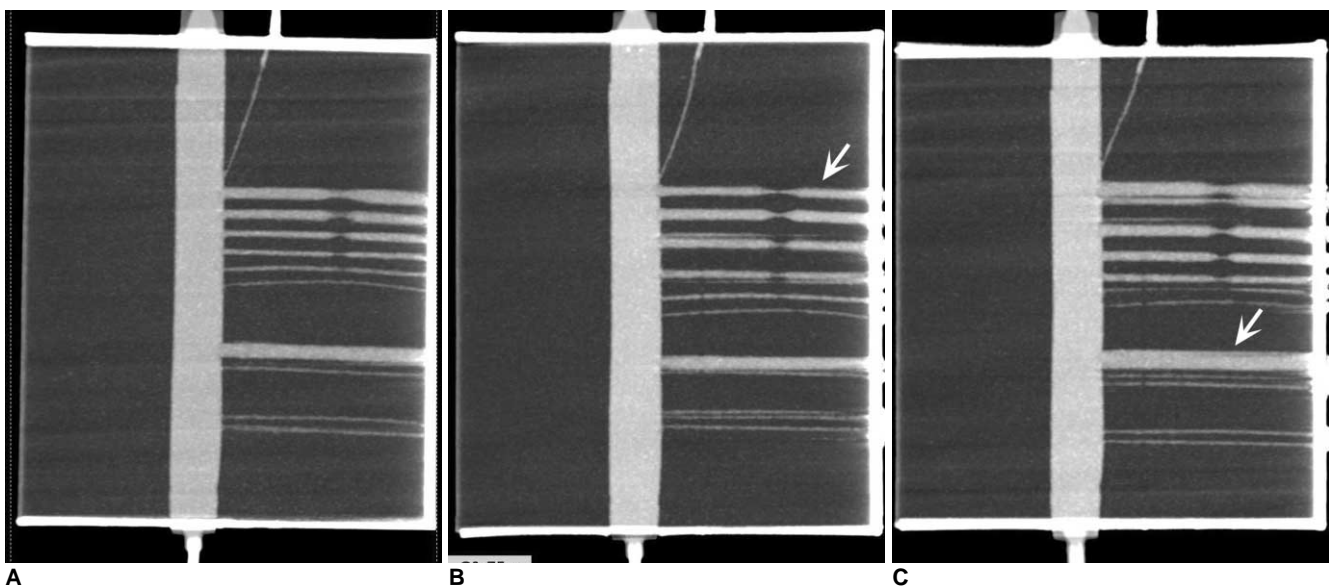
condition of amplitude 1 cm-20 RPM and amplitude 1 cm-40 RPM, the image quality improved constantly as the scanning speed increased (Fig. 6). The result can be explained by the relationship of the scanning speed and speed of phantom movement (Figs. 4, 5).

When the velocity of the phantom movement increased, the graphs of the averaged scores showed a different trend at the scan speed of 2.4 cm/sec (pitch 1.5 and gantry rotation time 0.75 sec) and the scanning speed of 3.2 cm/sec (pitch 1 and gantry rotation time 0.37 sec); the scanning speed at pitch 1–0.37 sec (3.2 cm/sec) was faster than for pitch 1.5–0.75 sec (2.4 cm/sec). For the condition of 3 cm–20 RPM, values of these two points did not show

much difference. With the faster phantom movement condition of 3 cm–40 RPM, the average score for the condition of pitch 1–0.37 sec was even lower than for the condition of pitch 1.5–0.75 sec.

Reversal of image quality with increased scanning speed during fast phantom movement cannot be explained only by the difference in the scanning speed or the velocity of phantom movement (10). The other factor that showed a difference between the aforementioned conditions is the movement of the detector of the CT machine (Table 5, Fig. 9). When the range of the scan was limited to only 1.8 cm for the convenience of calculation, for the condition of pitch 1.5–0.75 sec and 3 cm–40 RPM, it took 0.75 sec for


A **B** **C**

Fig. 8. Representative samples of motion artifact.
A. Image without distortion for condition of 4.8 cm/sec scanning speed (pitch 1.5 and gantry rotation 0.37 sec) and phantom movement of amplitude 1 cm-20 RPM. All of tubes show clear margins.
B. For condition of 2.4 cm/sec scanning speed (pitch 1.5 and gantry rotation 0.75 sec) and phantom movement of amplitude 1 cm-20 RPM, uppermost tube shows decreased diameter (white arrow) as compared to tube with same location in **A**. This is example of misregistration when phantom tubes moves faster than CT table in same direction. As velocity changed constantly, tubes with similar diameter showed different width on CT images.
C. For condition of 4.8 cm/sec scanning speed (pitch 1.5 and gantry rotation 0.37 sec) and phantom movement of amplitude 1 cm-40 RPM, seventh tube (white arrow) shows increased diameter as compared to tube with same location in **A**. This is example of misregistration when object moves slowly in opposite direction to that of CT table.

A **B**
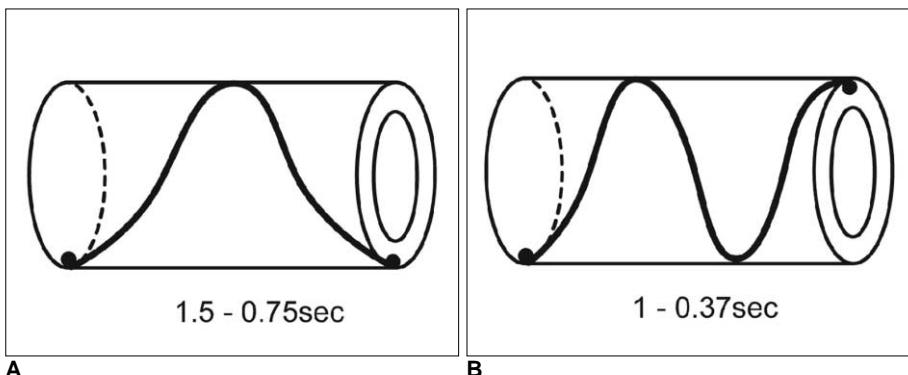
Fig. 9. Differences of gantry rotation angle per unit distance of 1.8 cm for each scan condition.
A. For condition of 1.5 pitch and 0.75 sec rotation time, gantry rotates 360° for 1.8 cm.
B. For condition of 1 pitch and 0.37 sec rotation time, gantry rotates 540° for 1.8 cm.

Table 5. Time and Rotation Angle of Gantry Per Unit Distance of 1.8 cm for Each Scan Condition

	Protocol (pitch-gantry rotation time)	
	1.5–0.75 sec	1–0.37 sec
Scan speed	2.4 cm/sec	3.2 cm/sec
Time/1.8 cm*	0.75 sec	0.55 sec
Rotation angle	360°	540°

Note.— Scanning range (*) was arbitrarily set for convenience of calculation.

the detector to move 1.8 cm; the gantry rotation angle was 360°. For the condition of pitch 1–0.37 sec and 3 cm–40 RPM with the same range of a scan it took 0.55 sec to move 1.8 cm, but the gantry rotation angle was approximately 540°. This finding showed that the detector traveled about 50% farther due to the shorter gantry rotation time. With the higher pitch, the detector was likely to obtain more information for the moving phantom, but the information overlapped and reconstructed images showed some degree of blurring. As for the average values and standard deviations of the largest tube without stenosis, the graphs also showed that a higher scanning speed improved the quality of the images.

It is generally known that when obtaining images with higher pitches, fine details of images get blurred. Details of small structures such as vessels with a small diameter cannot be clearly identified. When the object moves, artifacts caused by movement are another determinant of image quality. As the speed of an object is faster than some level, artifacts induced by movement are the main causes of poor image quality. According to this study, it is helpful to obtain images with a higher pitch in order to overcome motion artifacts (Fig. 6).

We acknowledge some limitations of our study. First, as the study was performed only with a 16-channel multi-detector row CT (MDCT) scanner, an imaging pitch of 2 was not possible due to the limitations of the CT unit. We expect that faster scans with the use of a 64-channel MDCT scanner may improve image quality. Second, as the time difference for synchronization of the gantry and phantom movement for each scan condition was not predictable; we tried to minimize the uncertainty by averaging the results from five separate scans. Third, *in vivo* motions of cardiovascular structures are three-dimensional and represent the summation of cardiac and respiratory motion. We considered only respiratory

motion for two-dimensional diaphragmatic movement. Fourth, movement of the phantom caused by the small ventilator did not reflect the *in vivo* time difference between inspiration and expiration; we thought that the time difference itself did not significantly contribute to a motion artifact.

In conclusion, the speed of scanning is a very important factor to improve image quality. However, when the time undertaken for scanning is similar or slightly different between conditions with different pitches and gantry rotation times, scanning with a higher pitch and longer gantry rotation time (i.e., 1.5–0.75 sec) provides better results as compared to a lower pitch and shorter gantry rotation time (1–0.37 sec).

References

1. Westra SJ, Hill JA, Alejos JC, Galindo A, Boechat MI, Laks H. Three-dimensional helical CT of pulmonary arteries in infants and children with congenital heart disease. *AJR Am J Roentgenol* 1999;173:109-115
2. Filipek MS, Gosselin MV. Multidetector pulmonary CT angiography: advances in the evaluation of pulmonary arterial diseases. *Semin Ultrasound CT MR* 2004;25:83-98
3. Suzuki S, Furui S, Kaminaga T, Yamauchi T. Measurement of vascular diameter in vitro by automated software for CT angiography: effects of inner diameter, density of contrast medium, and convolution kernel. *AJR Am J Roentgenol* 2004;182:1313-1317
4. Suzuki S, Furui S, Kaminaga T. Accuracy of automated CT angiography measurement of vascular diameter in phantoms: effect of size of display field of view, density of contrast medium, and wall thickness. *AJR Am J Roentgenol* 2005;184:1940-1944
5. Mahesh M, Scatarige JC, Cooper J, Fishman EK. Dose and pitch relationship for a particular multislice CT scanner. *AJR Am J Roentgenol* 2001;177:1273-1275
6. Silverman PM, Kalender WA, Hazle JD. Common terminology for single and multislice helical CT. *AJR Am J Roentgenol* 2004;176:1135-1136
7. Rubin GD, Shiau MC, Leung AN, Kee ST, Logan LJ, Sofilos MC. Aorta and iliac arteries: single versus multiple detector-row helical CT angiography. *Radiology* 2000;215:670-676
8. Cohen RA, Frush DP, Donnelly LF. Data acquisition for pediatric CT angiography: problems and solutions. *Pediatr Radiol* 2000;30:813-822
9. Ko SF, Hsieh MJ, Chen MC, Ng SH, Fang FM, Huang CC, et al. Effects of heart rate on motion artifacts of the aorta on non-ECG-assisted 0.5-sec thoracic MDCT. *AJR Am J Roentgenol* 2005;184:1225-1230
10. Ritchie CJ, Godwin JD, Crawford CR, Stanford W, Anno H, Kim Y. Minimum scan speeds for suppression of motion artifacts in CT. *Radiology* 1992;185:37-42